

PACS numbers: 42.81.Dp; 42.81.Wg; 42.65.Es
DOI: 10.1070/QE2010v040n10ABEH014389

Model of a fibreoptic phase-sensitive reflectometer and its comparison with the experiment

O. Tosoni, S.B. Aksenov, E.V. Podivilov, S.A. Babin

***Abstract*. A statistical model describing the Rayleigh-scattering reflectograms of narrowband Gaussian pulses in optical fibres is constructed taking into account linear (the finite spectral linewidth because of frequency fluctuations, finite frequency band of the photodetector) and nonlinear (modulation instability) effects influencing the reflectograms' visibility. The model is compared with the experiment, demonstrating the adequacy of the theoretical description. The possibilities of obtaining optimal parameters, important for practical applications of the phase-sensitive reflectometer as a distributed fibreoptic intrusion sensor are discussed.**

Keywords: *phase-sensitive reflectometer, intruder alarm system, Rayleigh scattering.*

1. Introduction

For more than thirty years the optical time domain reflectometry has been used to detect defects in optical fibres [1]. This technique employs transmission of short light pulses in an optical fibre and examination of their reflectograms, i.e., the time dependence of the Rayleigh-scattering signal power in the direction opposite to that of pulse propagation. In conventional reflectometers low-coherent probing radiation (with a broad spectrum) is used to suppress interference effects and eliminate unwanted fluctuations. Such systems are characterised by temporal exponential attenuation of the scattered signal power in accordance with the distance propagated by the pulse [2]. In a phase-sensitive reflectometer we get, by contrast, the coherent effects amplified and observe those power fluctuations which are avoided in conventional reflectometers (this requires radiation from a narrowband probe laser [3]). Phase-sensitive reflectometers are used to design intrusion sensors whose high sensitivity is ensured by the interference character of the observed signal (see, for example, [3, 4]).

Rayleigh scattering from the refractive-index inhomogeneities in an optical fibre was thoroughly studied theoretically by using the equations for the electromagnetic fields in the fibre [5, 6]. It was shown that a part of scattered light excites the waveguide mode and counterpropagates in the fibre, while the other part is lost. The fraction of backward scattering compared to the total Rayleigh loss is determined by the 'recapture' coefficient S, which is of the order of 0.1 % – 1 %. To describe not only the average power of scattered light but also the fine structure of the reflectograms, the authors of paper [7] developed a more detailed statistical approach, which, however, neglected the nonlinear effects, in particular, development of the modulation instability, which plays an important role when high-power (both pico- and nanosecond [8, 9]) pulses propagate in the region of anomalous group-velocity dispersion ($\lambda \gg 1.4$ μm for a single-mode fibre).

The aim of this paper is to simulate and analyse in detail the properties of scattered light, taking into account the experimental parameters. The paper describes the experimental setup and the obtained results, as well as presents the theory and the data on the numerical simulation of the reflectograms by neglecting the nonlinear effects, which are considered separately.

2. Experimental

The experimental setup, similar to that described in [4] and [9], consists of a coherent pulsed radiation source and a single-mode fibre (Fig. 1). The source is a pulsed laser diode, which is frequency-stabilised by the fibre Bragg grating (FBG) and emits 1550-nm pulses with a pulse repetition rate of 833 Hz. Radiation from the diode is coupled into two erbium-doped fibre amplifiers. The length of the active fibre in the first amplifier is 2 m, while in the second – 6 m. The peak power of the laser diode is about 1 mW, and the output power of the second amplifier can vary from 1 to 16 W. Most of the broadband noise signal (amplified spontaneous emission) is cut off by the FBG filters, mounted behind each segment of the active fibre of the amplifier. Output radiation from the second amplifier is delivered to the 20-km-long probe fibre, while the back-scattered signal is fed, via the circulator, to the photodetector connected to an oscilloscope.

O. Tosoni Novosibirsk State University, ul. Pirogova 2, 630090 Novosibirsk, Russia; e-mail: olivier.tosoni@polytechnique.edu;
S.B. Aksenov Institute of Automation and Electrometry, Siberian Branch, Russian Academy of Sciences, prosp. akad. Koptyuga 1, 630090 Novosibirsk, Russia;
E.V. Podivilov, S.A. Babin Novosibirsk State University, ul. Pirogova 2, 630090 Novosibirsk, Russia; Institute of Automation and Electrometry, Siberian Branch, Russian Academy of Sciences, prosp. akad. Koptyuga 1, 630090 Novosibirsk, Russia; e-mail: babin@iae.nsk.su

Received 1 July 2010
Kvantovaya Elektronika **40** (10) 887 – 892 (2010)
Translated by I.A. Ulitkin

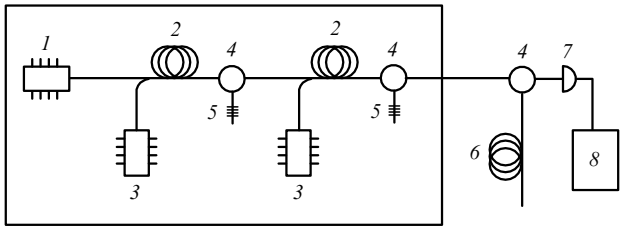

Figure 1. Scheme of the experimental setup: (*1*) pulsed laser diode ($\lambda = 1550$ nm); (*2*) active erbium-doped fibres; (*3*) laser diodes pumping fibre amplifiers ($\lambda = 980$ nm); (*4*) fibre circulators; (*5*) Bragg gratings for spectral filtration (1550 nm); (*6*) 20-km-long probe (passive) fibre; (*7*) photodetector; (*8*) oscilloscope.

Figure 2 shows a typical experimental reflectogram. One can clearly see the resolved power fluctuations near the average value, which decreases because of losses in accordance with the known exponential law $I(z) = I(0)\,\mathrm{e}^{-2\alpha z}$. The experimental (0.20 dB km^{-1}) and nominal (0.19–0.20 dB km^{-1}) loss coefficients for this fibre almost coincide. The characteristic feature of the reflectogram's fluctuations is the visibility, i.e. the ratio of the standard power deviation σ from its average value to the average value itself:

$$\eta(t) = \frac{\sigma(I(t))}{\langle I(t)\rangle}. \tag{1}$$

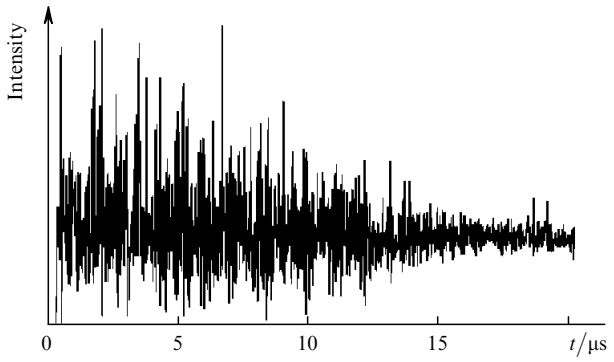

Figure 2. Reflectogram obtained with a photodetector ($T_\mathrm{i}^{-1} =$ 100 MHz) from 50-ns, 2-W pulses.

In the presented reflectogram, the visibility equal to ~ 40 % decreases down to 9 % within the first microseconds (i.e., for the several hundreds of meters of the fibre). It is found that the reflectogram's visibility depends on the photodetector frequencies and on the pulse power. The theoretical model presented below allowed us to estimate the visibility both analytically and numerically as well as to find the optimal parameters needed to obtain reflectograms with maximal visibility.

3. Analytic model and numerical calculations

3.1 Model

We used the statistical model [7] to describe theoretically the reflectograms: each small segment of a fibre of length Δl has an effective back-reflection coefficient $\Delta\rho(z)$. The reflected-wave amplitude at the fibre input is expressed by the integral along its entire length from all the partial contributions of reflection from different points z:

$$E(t) = \sqrt{I_0}\int_0^L f\left(t - \frac{2z}{v}\right)\exp\left[\mathrm{i}\phi\left(t - \frac{2z}{v}\right)\right]\rho(z)\mathrm{d}z. \tag{2}$$

Here, we introduced a random quantity

$$\rho(z) = \lim_{\Delta l\to 0}(\Delta\rho(z)/\Delta l),$$

i.e., a differential backscattering coefficient whose distribution is assumed Gaussian and delta-correlated:

$$\langle\rho^*(z_1)\rho(z_2)\rangle = 2\sigma^2\delta(z_1 - z_2), \tag{3}$$

where $2\sigma^2 = \alpha_\mathrm{s}S$ is the product of the Rayleigh-scattering coefficient α_s by the recapture coefficient S calculated in [5]; v is the speed of light in a fibre. The function $f(th)$ is the pulse profile normalised to the maximum and having the effective duration T ($\int|f(t)|^2\mathrm{d}t = T$); $\phi(t)$ describes the phase noise of the laser source. Equations (2) and (3) are basic in further calculations.

The authors of paper [7] showed that the visibility of the reflectogram's fluctuations (which we will further call simply visibility) is theoretically equal to unity in the cw regime when polarisation effects are neglected. However, because of the finiteness of the response time of a measuring device the experimental visibility can be smaller: it is impossible to measure fast power fluctuations with a slow detector.

The power I_exp measured by the device is expressed by an integral in the instantaneous power $I(t)$ over some time interval T_i (the detector's response time):

$$I_\mathrm{exp}(t) = \frac{1}{T_\mathrm{i}}\int_0^{T_\mathrm{i}} I(t + t')\mathrm{d}t'. \tag{4}$$

The observed visibility is a ratio of the standard deviation I_exp to the average power:

$$\eta^2 = \frac{\sigma^2_{I_\mathrm{exp}}}{\langle I\rangle^2} = \frac{\langle I^2_\mathrm{exp}\rangle - \langle I_\mathrm{exp}\rangle^2}{\langle I\rangle^2}, \tag{5}$$

where

$$\langle I\rangle = 2\sigma^2\frac{vT}{2}I_0; \tag{6}$$

$$\langle I_\mathrm{exp}(t)^2\rangle = \frac{1}{T_\mathrm{i}^2}\int_0^{T_\mathrm{i}}\int_0^{T_\mathrm{i}} R(t' - t'')\,\mathrm{d}t'\mathrm{d}t'' \tag{7}$$

is expressed by the correlation function of the reflected signal

$$R(t,\tau) = \langle I(t)I(t+\tau)\rangle. \tag{8}$$

In the cw regime, η is independent of time t. Gysel et al. [7] showed that for an infinitely long fibre and a Lorentzian spectral linewidth $\Delta\omega$, the correlation function has the form:

$$R(\tau) = \langle I\rangle^2(1 + \mathrm{e}^{-\Delta\omega|\tau|}). \tag{9}$$

Substituting (9) into (7) and (7) into (5), we obtain the

dependence of the visibility on the detector response time T_i and on the spectral linewidth $\Delta\omega$ of the radiation source:

$$\eta = \left\{ \frac{2}{(T_i\Delta\omega)^2}\left[e^{-T_i\Delta\omega} - (1 - T_i\Delta\omega)\right]\right\}^{1/2}. \quad (10)$$

At $T_i \to 0$ we have $\eta \to 1$, and at large $T_i\Delta\omega$, the visibility η decreases according to the root law.

Strictly speaking, for short pulses of duration T comparable with $(\Delta\omega)^{-1}$, formula (10) is modified. But we show in the Appendices that formula (10) can be used in the pulsed regime.

In the experiment the reflectogram's visibility was measured by sensors with the response time $T_i^{-1} = 100$, 10, 1, and 10^{-3} MHz, and then was compared to the theoretical curve (Fig. 3). As the direct measurement of the laser linewidth $\Delta\omega$ was impossible, because it was much smaller that the spectral resolution of the optical analyser, we measured the coherence length of the laser with a fibre interferometer. Then we used the coherence length to find the spectral linewidth. The measured value was $l_{coh} \approx 3$ m; therefore, $\Delta\omega \approx 150$ MHz. The inaccuracy of this method is rather large – Fig. 3 shows the measurement uncertainty at each point. Taking into account the estimated errors, the agreement between theory and experiment is satisfactory.

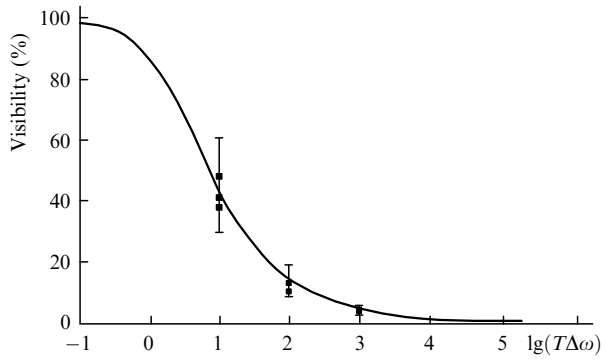

Figure 3. Reflectograms' visibility obtained theoretically (curve) and measured by 100-, 10-, 1-, and 10^{-3}-MHz photodetectors (points). The vertical segments correspond to the error in measuring the width $\Delta\omega$ of the master laser. Each detector was used for several measurements.

Note that the accuracy in measuring the laser linewidth can be increased if we use (as in paper [4]) a scanning fibre interferometer.

3.2 Numerical simulation

To test the adequacy of the model, we performed numerical calculations. The window τ used in calculations exceeded the pulse duration T by five times. It was divided into N identical segments of duration τ/N inside which the amplitude f_k was assumed constant. For a Gaussian pulse, we have

$$f_k = \exp\left[-r^2\left(\frac{k}{N} - \frac{1}{2}\right)^2\right]. \quad (11)$$

The observation period t_{max} was chosen so that the theoretical reflectogram consist of $M = Nt_{max}/\tau$ points. Random scattering centres were simulated by $(N + M)$-component vector R_k of independent complex random quantities taken from the distribution (proposed in [7]):

$$D_k = \mathcal{N}(0,1)\exp\{i\mathcal{U}([0,2\pi])\}. \quad (12)$$

Power fluctuations of the master laser during the pulse action were set by the N-component vector Φ_k as

$$\Phi_0 = 0, \quad (13)$$

$$\Phi_{k+1} = \Phi_k \exp\left[i\frac{T}{n}\mathcal{L}\left(0, \frac{\Delta\omega}{2}\right)\right].$$

$\mathcal{N}(0,1)$, $\mathcal{U}([0,2\pi])$, and $\mathcal{L}(0,\Delta\omega/2)$ were used to designate random quantities with normal (average deviation, 0; standard deviation, 1), uniform, and Lorentz distributions, respectively. For the kth $(k = 1,...,M)$ point of the reflectogram, we have

$$p_k = \sum_{l=1}^{N} f_l\,\Phi_l\,D_{k+l-1}. \quad (14)$$

The finiteness of the photodetector band is taken into account in accordance with (4): the number $n_i = T_iN/\tau$ of successive points that should be summed up, corresponds to the response time T_i. Figures 4 and 5 compare the reflectograms obtained numerically and experimentally with a pulsed laser emitting 50-ns pulses at a pulse repetition rate of 150 MHz. We determined the following values of the visibility:

(i) with a slow photodetector ($T_i^{-1} = 10$ MHz): $\eta_{exp} = 10\,\% - 13\,\%$, $\eta_{theor} = 14\,\%$ and $\eta_{numer} = 17\,\%$;

(ii) with a fast photodetector ($T_i^{-1} = 100$ MHz): $\eta_{exp} = 38\,\% - 49\,\%$, $\eta_{theor} = 42\,\%$ and $\eta_{numer} = 45\,\%$.

Taking into account the random character of the reflectograms, the obtained inaccuracy is quite acceptable.

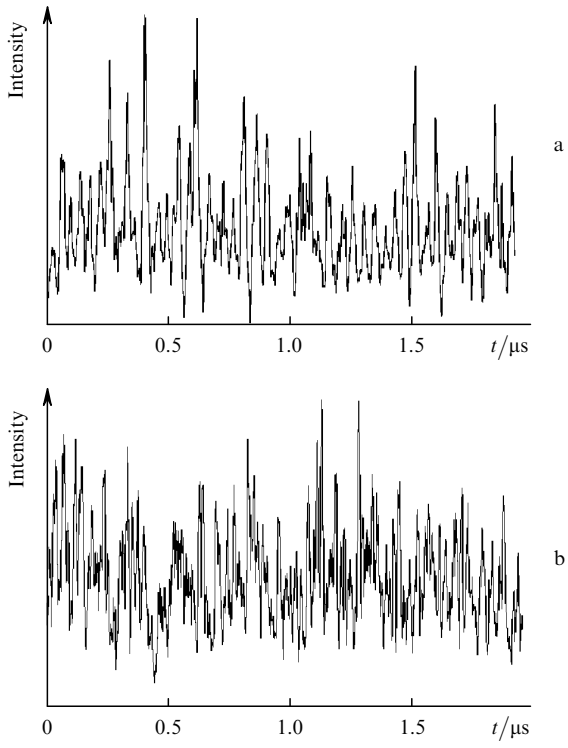

Figure 4. Results of the experiment (a) and simulation (b) with a fast photodetector.

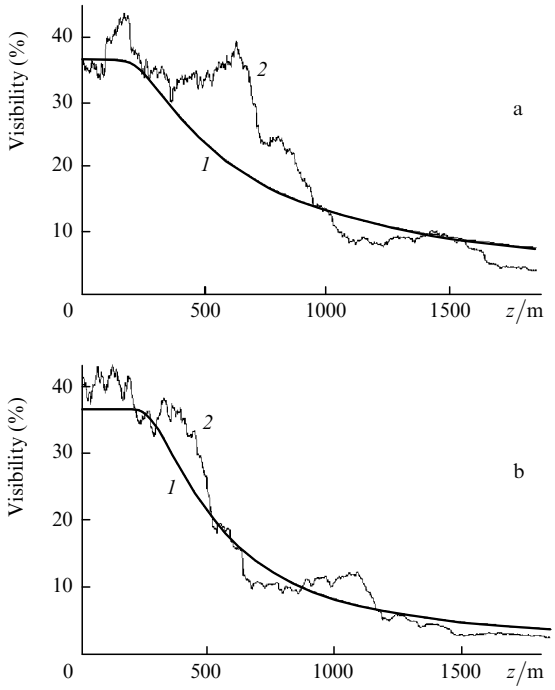

Figure 5. Dependences of the calculated (*1*) and experimental (*2*) visibility on the distance to the reflection point z at $I_0 = 1.9$ W (a) and 5.2 W (b).

3.3 Polarisation

As was shown in [7], the presence of birefringence in optical fibres can help decrease the visibility: thus, in circular fibres random rotation of polarisation when radiation propagates in the fibre reduces visibility down to 0.5. The reason behind this is the beatings of the polarisation components, preventing the appearance of complete interference.

However, the spatial scale of beatings l_b is usually equal to several hundreds of meters, while the pulse duration in our case is 10 m. Thus, the field components on the pulse scale have no time to move; therefore, neglect of polarisation effects in our model is justified.

4. Effect of the modulation instability

It is known that in the case of anomalous group-velocity dispersion there can appear a nonlinearity-induced modulation instability [8], which leads to a strong spectral broadening of narrowband pulses at high pulse powers. The relationship between the narrowband and broadband (caused by the noise produced by the amplifiers) parts of the pulse spectrum changes as the pulse propagates in the fibre. We will not consider here the phenomenon of the modulation instability of nanosecond pulses, which was thoroughly studied in [9], but will analyse the manifestation of the modulation instability in the reflectograms.

If the spectrum of input radiation consists of two spectral components having different linewidths with weights a_n and a_w, then taking into account the fact that the spectral power density is a Fourier transform of correlation function (8), we can show that the reflectogram's visibility is expressed as a function of visibility, which would have been obtained from each contribution – narrowband (η_n) and broadband (η_w) – separately:

$$\eta_{sum} = (a_n \eta_n^2 + a_w \eta_w^2)^{1/2}. \tag{15}$$

The widths of the narrowband and broadband parts are, respectively, 1 GHz and 700 GHz, i.e., the products $T_i\Delta\omega_n$ and $T_i\Delta\omega_w$ in the case of a fast photodetector (100 MHz) are 10 and 7000, respectively. For such large $\Delta\omega T_i$ we can use the approximation $\eta_i = (2/T_i\Delta\omega_i)^{1/2}$ instead of (10).

Let us estimate the fraction of the narrow- and broadband spectral components a_n and a_w by the experimental data given in paper [9].

(i) During pulse propagation the power of the broadband part grows exponentially until the level, comparable with the narrowband part of the spectrum, is reached. The exponent held coefficient is proportional to the initial peak power such that

$$a_w(I_0, z) \sim e^{vI_0 z}, \tag{16}$$

where the parameter $v \approx 5.3$ W^{-1} km^{-1} is proportional to the fibre nonlinearity coefficient.

(ii) The characteristic length for which the exponential growth stops depends according to the logarithmic law on the initial ratio of the powers of both components, the ratio being approximately equal to the relative pulse duration [9].

(iii) For distances z exceeding the characteristic length, we can present only the numerical results from [9]. It follows from these results that the power of the narrowband component decreases as z^{-2}.

As a result, to simulate the visibility we can approximate a_n and a_w by the functions:

$$a_w(z) = \exp\left[-\left(\frac{\ln \alpha_d}{vI_0 z}\right)^2\right],$$
$$a_n(z) = 1 - a_w(z). \tag{17}$$

The losses resulting from pulse propagation at distances of 1–2 km can be neglected.

Figure 5 demonstrates experimental and calculated values of the visibility as a function of z at two initial peak pulse powers. The experimental visibility was estimated by the running window of 100 successive experimental points from the reflectograms obtained at different input powers.

5. Discussion

5.1 Optimal characteristics of the source

The obtained results make it possible to determine the optimal parameters of phase-sensitive intrusion sensors:

(i) narrow spectrum of the master laser as well as a fast and sensitive photodetector, required to fulfil the relation $T_i\Delta\omega \leqslant 1$;

(ii) peak power no more than ~ 1 W to circumvent the development of the modulation instability [9];

(iii) ~ 50-ns pulse duration ensuring, on the one hand, a satisfactory spatial resolution of ~ 5 m and, on the other hand, – sufficient reflected-signal power for the above limitation on the pulse power.

5.2 Effect of stimulated inelastic scattering

Nonlinear processes such as stimulated inelastic scattering are characterised by the fact that they rigidly limit the peak powers of optical signals. The author of [10] presented the

estimates of the power threshold for Raman and Brillouin processes:

(i) The Raman amplification spectrum is very wide, but the gain is small; therefore, the power threshold in a fibre of length L_{eff} is

$$P_{\text{th}}^{(\text{R})} L_{\text{eff}} \approx 50 \text{ W km}. \tag{18}$$

Because in our case the pulse duration is of the order of 10 m, this process does not limit the input power.

(ii) The Brillouin amplification spectrum is very narrow (a few tens of MHz), but the gain is much higher than the Raman one. If the pulse spectrum is rather narrow, we have

$$P_{\text{th}}^{(\text{B})} L_{\text{eff}} \approx 0.1 \text{ W km}; \tag{19}$$

therefore, for 50-ns pulses, $P_{\text{th}}^{(\text{B})} \approx 20$ W. At this power, the modulation instability significantly distorts the signal and hence the Brillouin scattering does not introduce any additional limitations. However, because radiation is back-scattered, we should insert an insulator in front of the radiation source in order not to damage it.

6. Conclusions

Thus, using the statistical model [7] and neglecting the polarisation effects, we have presented theoretical description of the Rayleigh-scattering reflectograms of nanosecond Gaussian laser pulses, taking into account the finite values of the frequency fluctuations of the laser spectrum $\Delta\omega$ and the response time of the photodetector T_{i} in the linear regime. We have compared the model with the experimental reflectograms at pulse durations $T \approx 50 - 150$ ns, the spectral width $\Delta\omega \approx 150$ MHz, and the photodetector bandwidth T_{i}^{-1} in the range from 1 kHz to 100 MHz, and obtained a satisfactory agreement. In addition, we have analysed the influence of nonlinear effects on the reflectogram. We have shown that with the wavelength range 1.5 μm fitting into the anomalous group-velocity dispersion region of a standard SMF-28 fibre, the main effect leading to a decrease in the reflectogram's visibility is the modulation instability developing because of the influence of the broadband noise from erbium-doped fibre amplifiers [9]. We have derived simple estimation formulae describing a nonlinear decrease in the visibility.

The constructed model makes it possible to calculate the reflectograms at the given parameters of the system and to optimise them in the experiments, which is important for designing phase-sensitive Rayleigh intrusion sensors.

Acknowledgements. The authors thank I.S. Shelemba, N.S. Tarasov, and A.G. Kuznetsov for technical assistance. This work was supported by the State Contract of the Ministry of Education and Science and the Integration Project of the Siberian Branch of the Russian Academy of Sciences.

Appendix 1

Scattered radiation spectrum

Let us derive the formulae for the reflected light spectrum when the cw laser has a Lorentzian spectral linewidth $\Delta\omega$ at half-height and the pulses have a Gaussian form with the width T.

We will start by calculating the correlation function. From the initial expression

$$\begin{aligned} R(t, t+\tau) &= \langle I(t)\rangle^2 + (2\sigma^2 I_0)^2 \\ &\times \left\{ \int_0^L \int_0^L f\left(t - \frac{2z_1}{v}\right) f\left(t+\tau - \frac{2z_1}{v}\right) \right. \\ &\times f\left(t - \frac{2z_3}{v}\right) f\left(t+\tau - \frac{2z_3}{v}\right) \\ &\times \left\langle \exp\left[-\mathrm{i}\phi\left(t - \frac{2z_1}{v}\right) + \mathrm{i}\phi\left(t+\tau - \frac{2z_1}{v}\right) \right.\right. \\ &\left.\left. \left. + \mathrm{i}\phi\left(t - \frac{2z_3}{v}\right) - \mathrm{i}\phi\left(t+\tau - \frac{2z_3}{v}\right)\right]\right\rangle \mathrm{d}z_1 \mathrm{d}z_3 \right\} \end{aligned} \tag{A1.1}$$

we obtain

$$R(\tau) = \langle I\rangle^2 \left[1 + \exp\left(-\frac{\tau^2}{2T^2}\right) J\left(T\Delta\omega, \frac{|\tau|}{\Delta t}\right)\right], \tag{A1.2}$$

where

$$\begin{aligned} J(p,q) &= \left(\frac{2}{\pi}\right)^{1/2} \left(\mathrm{e}^{-pq} \int_q^\infty \mathrm{e}^{-z^2/2} \mathrm{d}z \right. \\ &\left. + \mathrm{e}^{p^2/2} \int_p^{p+q} \mathrm{e}^{-z^2/2} \mathrm{d}z \right). \end{aligned} \tag{A1.3}$$

The time dependence t vanishes if we neglect the attenuation and edge effects from the fibre ends, i.e., when $t \gg \tau$.

The reflected-signal spectrum is given by the Fourier transform of function (A1.1), which is is expressed with good accuracy by the sum of two contributions:

$$\begin{aligned} S_{\text{rs}}(w) &\approx c(u) \frac{1}{\sqrt{2\pi}} \exp\left[-\frac{(\omega T)^2}{2}\right] \\ &+ [1 - c(u)] \frac{\tilde{u}}{\pi} \frac{1}{\tilde{u}^2 + (\omega T)^2}, \end{aligned} \tag{A1.4}$$

where

$$u = T\Delta\omega; \tag{A1.5}$$

$$c(u) = \left(\frac{2}{\pi}\right)^{1/2} \int_0^\infty \exp\left[-\frac{z(2u+z)}{2}\right] \mathrm{d}z; \tag{A1.6}$$

$$\tilde{u} \equiv \frac{u}{1 - c(u)}. \tag{A1.7}$$

The function $c(u) \to 1$ at $u \to 0$ and decreases as $\sqrt{2/\pi}\, u^{-1}$ at $u \to \infty$. The parameter u here is determining: the condition $u \ll 1$ corresponds to a narrowband laser, and in this case the Gaussian pulse determines the reflected-signal spectrum in time. In the limit $u \gg 1$, the pulse shape virtually does not affect the spectrum.

Appendix 2

General character of formula (10)

In the limit of long pulses ($T\Delta\omega \gg 1$), we have obtained the function describing the visibility versus the Lorentzian spectral linewidth of the master laser and the photodetector response time:

$$\eta = \left\{ \frac{2}{x^2} \left[e^{-x} - (1 - x) \right] \right\}^{1/2} = F_{\text{long}}(x), \tag{A2.1}$$

where

$$x = \Delta\omega T_{\text{i}}. \tag{A2.2}$$

For short Gaussian pulses ($T\Delta\omega \approx 1$), the spectrum is also Gaussian and the irregular character is expressed by the function

$$F_{\text{short}}(x) = \left\{ \frac{2}{x^2} \left[\exp\left(-\frac{x^2}{2} \right) - 1 + \sqrt{\frac{\pi}{2}} x \operatorname{erf}\left(\frac{x}{\sqrt{2}} \right) \right] \right\}^{1/2}, \tag{A2.3}$$

where

$$x = T_{\text{i}}/T. \tag{A2.4}$$

Comparing the plots of these two functions, we can see that they are close, which means that in both cases we can use a simpler function F_{long} (A2.1). Obviously, this result suits any intermediate distributions.

References

1. Barnovski M.K., Jensen S.M. *Appl. Opt.,* **15**, 2112 (1976).
2. Healey P. *J. Lightwave Technol.*, **LT-3**, 4 (1985).
3. Juarez J.C., Maier E.W., Choi K.N., Taylor H.F. *J. Lightwave Technol.*, **23**, 6 (2005).
4. Gorshkov B.G., Paramonov V.M., Kurkov A.S., Kulakov A.T., Zazirnyi M.V. *Kvantovaya Elektron.*, **36**, 963 (2006) [*Quantum Electron.*, **36**, 963 (2006)].
5. Brinkmeyer E. *Opt. Soc. Am.,* **70**, 8 (1980).
6. Nakasawa M. *Opt. Soc. Am.,* **73**, 9 (1983).
7. Gysel P., Staubli R.K. *J. Lightwave Technol.*, **8**, 4 (1990).
8. Tai K., Hasegawa A., Tomita A. *Phys. Rev. Lett.,* **56**, 2 (1986).
9. Ismagulov A.E., Babin S.A., Podivilov E.V., Fedoruk M.P., Shelemba I.S., Shtyrina O.V. *Kvantovaya Elektron.*, **39**, 765 (2009) [*Quantum Electron.*, **39**, 765 (2009)].
10. Agrawal G.P. *Fiber-Optic Communication Systems* (New York: Wiley, 1997).